Electronic Materials Letters, Vol. 6, No. 4 (2010), pp. 193-199
DOI: 10.3365/eml.2010.12.193 Published 31 December 2010

Thermoelectric Properties of $(ZnSb)_{1-x}$-$(MSb)_x$ Binary Systems

Kyung-Wook Jang,[1,*] Han-Jun Oh,[1] In-Ki Kim,[1] Il-Ho Kim,[2] and Jung-Il Lee[2]

[1]Department of Advanced Materials Engineering, Hanseo University,
360 Daegok-ri, Haemi-myeon, Seosan-si, Chungnam 356-706, Korea
[2]Department of Materials Science and Engineering, Chungju National University,
50 Daehangno, Chungju-si, Chungbuk 380-702, Korea

This study examines the formation of a solid solution and the thermoelectric properties of $(ZnSb)_{1-x}$-$(MSb)_x$ binary systems, where M is In or Ga. In ZnSb-GaSb systems, X-ray diffraction peaks for GaSb appear at GaSb concentrations greater than 3 mol. % but not for GaSb concentrations of less than 1 mol. %. As the molecular percentage of GaSb is increased, the electrical conductivity, thermal conductivity, and carrier concentration of ZnSb-GaSb systems increase, but the mobility and Seebeck coefficient decrease. The ZT value reaches a maximum of 0.03 in ZnSb-10 mol. %GaSb at 623 K. The Seebeck coefficient of ZnSb-InSb systems appears to have no linear relation with the level of InSb addition. The electrical conductivity decreases as the Seebeck coefficient increases. The thermoelectric power factor of ZnSb-InSb systems reaches a maximum of 0.7 $mWm^{-1}K^{-2}$ at 623 K in ZnSb-10 mol. %InSb.

Keywords: ZnSb, thermoelectric, hall effect

1. INTRODUCTION

Zinc antimonides such as Zn_4Sb_3 and ZnSb are well-known thermoelectric materials; they have a high potential as the p-type leg of thermoelectric couples and are used to generate electrical power in a temperature range of 300 K to 700 K. The thermoelectric power factor of ZnSb is high enough to make it an attractive thermoelectric material.[1] However, the relatively high thermal conductivity of ZnSb needs to be reduced in order to improve the thermoelectric conversion efficiency.

A number of studies have examined the properties of the single crystals of ZnSb.[2,3] Other studies[4,5] have focused on reducing the lattice thermal conductivity through the formation of a substitutional solid solution between ZnSb and CdSb and on producing n-type semiconductors through doping with Te and so on. Recently, Schlecht and Mann[6] examined the synthesis of nanometer-sized powder and the plating of nanocluster films of ZnSb; however, there are no reports on the thermoelectric properties.[7] The thermoelectric properties of ZnSb films deposited by means of metalorganic chemical vapor deposition[8] and ionized cluster beam deposition indicate that a dimensionless figure of merit (ZT) of approximately 5 at 520 K can be expected. This expectation is based on the assumption that the thermal conductivity of the ZnSb thin films deposited by means of ionized cluster beam deposition is comparable to that of bulk poly-crystalline samples. ZT is defined as $ZT = \alpha^2\sigma T/\kappa$, where α is the Seebeck coefficient, σ is the electrical conductivity, κ is the thermal conductivity, and T is the temperature in Kelvin.

Phonon scattering from a substitutional solid solution is one of the most effective ways of reducing thermal conductivity. Semiconducting materials that form solid solutions are particularly interesting systems, especially in the way the properties vary smoothly with the composition.[9] This capability makes it possible to select the optimum composition. Almin *et al*. suggested that ZnSb and CdSb have an orthorhombic structure in the space group, D^{15}_{2h}-P/bca.[10,11] In addition, CdSb forms a pseudo-binary solid solution with ZnSb over the entire composition range.[12] We recently confirmed that the thermal conductivity of ZnSb is reduced, as shown in Fig. 1, by the solid solution forming effect of CdSb with ZnSb.[4] On the other hand, GaSb and InSb are also known to have the same crystal structure, which suggests they may form pseudo-binary solid solutions with ZnSb. This study examines the possibility of the solid solution formation of GaSb-ZnSb and ZnSb-InSb; it also examines how GaSb and InSb alloying at concentrations of up to 50 mol. % affects the thermoelectric properties of ZnSb at temperatures between 323 K and 623 K.

2. EXPERIMENTAL PROCEDURE

Ingots of ZnSb-GaSb and ZnSb-InSb with 1 mol. % to 50

*Corresponding author: kwjang@hanseo.ac.kr

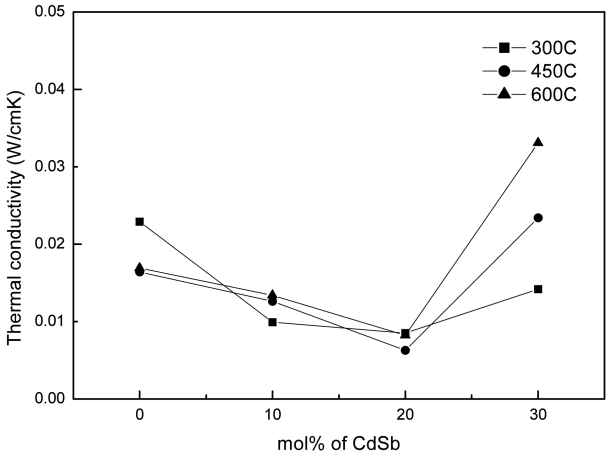

Fig. 1. CdSb alloying effect on the thermal conductivity of pseudo-binary ZnSb-CdSb solid solutions.

mol. % of GaSb and InSb, respectively, were prepared by melting high purity (99.99%) elemental Zn, Ga, In, and Sb pieces at 1173 K in a graphite mold that was first sealed in a quartz ampoule evacuated to 10^{-3} Torr, and then quenched in water. Melt quenching is generally used to produce a more uniform composition in the ingots but can lead to considerably more macro-cracks and micro-cracks, or even large voids, in the ingots. A graphite mold has a larger thermal expansion coefficient than a quartz tube and is effective in preventing the type of crack formation that occurs when the volume expands during a cooling phase. Each ingot has an upper diameter of 10 mm and a lower diameter of 5 mm. Subsequent isothermal annealing was conducted at 673 K for 24 h in a vacuum to ensure homogeneous microstructures.

Most of the measurements were taken from dense polycrystalline samples cut from the ingots. The phases of the annealed specimens were analyzed with the aid of an X-ray diffractometer (XRD: Rigaku RINT2000) using Cu K_α radiation. The microstructure was examined with a scanning electron microscope (SEM: JEOL JSM-5600), and the composition was analyzed with an energy dispersive X-ray spectroscope (EDS). The Seebeck coefficient and electrical conductivity were determined by means of a differential temperature method and a four-probe method (Ulvac-Rico ZEM2-M8) in the range of 323 K to 623 K. The thermal conductivity was calculated with the equation $k = aCd$, where a is the thermal diffusivity, C is the specific heat, and d is the density. A laser flash method (Ulvac-Riko TC7000) was used to measure the properties. The dimensionless thermoelectric figure of merit (ZT) was evaluated from the measured thermoelectric properties. The Hall coefficient was measured to determine the carrier concentration and mobility under conditions of a magnetic field (1 T) and electric current (50 mA) at room temperature.

3. RESULTS AND DISCUSSION

3.1. Microstructures

Figs. 2 and 3 show XRD patterns of the ZnSb-GaSb and ZnSb-InSb systems, respectively. In the ZnSb-GaSb systems, the diffraction peaks for GaSb were observed at GaSb concentrations greater than 3 mol. % but not for GaSb concentrations of less than 1 mol. %. Figs. 4(a) and (b) show the microstructural differences of the samples shown in Fig. 2. In the case of 1 mol. % GaSb, only Zn and Sb were detected with an EDS. However, in ZnSb-3 mol. %GaSb, GaSb phases formed between the ZnSb compound phases. The ZnSb phase peaks shifted slightly to a lower angle, which suggests that a small amount of GaSb dissolved in the ZnSb. This behavior suggests that the solubility of GaSb in the ZnSb-GaSb system is around 3 mol. %. On the other hand, the solubility limit in the ZnSb-InSb system, where the diffraction peaks for the ZnSb and InSb compound are present in ZnSb-2mol. %InSb, could not be determined due to the limited information. A metallic Sb phase was also detected in both systems. To date, no reliable method of synthesizing ZnSb crystals with a uniform composition and sufficiently perfect structure has been found because ZnSb crystallizes from melts via a peritectic reaction.[13]

Figures 4 and 5 show SEM images of the ZnSb-GaSb and ZnSb-InSb systems, respectively. For ZnSb-1 mol. %GaSb, no GaSb phase can be identified from the SEM images and EDS analysis. The volume fractions of each compound phase increase as the GaSb and InSb mole percentages increase. In ZnSb-5 mol. %GaSb, the ZnSb phase appears initially in the form of primary crystals from the melt; the remaining melt is solidified by a eutectic-like reaction, as shown in Fig. 4(c). In ZnSb-40 mol. %GaSb, on the other hand, the primary GaSb phase crystallizes from the melt and the GaSb and ZnSb phases appear to solidify simultaneously

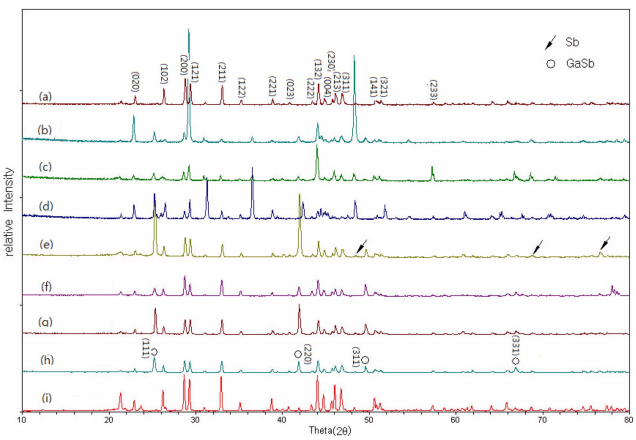

Fig. 2. X-ray diffraction patterns of the ZnSb-GaSb systems ; (a) ZnSb, (b) 5 mol. % GaSb, (c) 3 mol. % GaSb, (d) 1 mol. % of GaSb, (e) 10 mol. % of GaSb, (f) 20 mol. % GaSb, (g) 30 mol. % GaSb, (h) 40 mol. % of GaSb, and (i) 50 mol. % of GaSb.

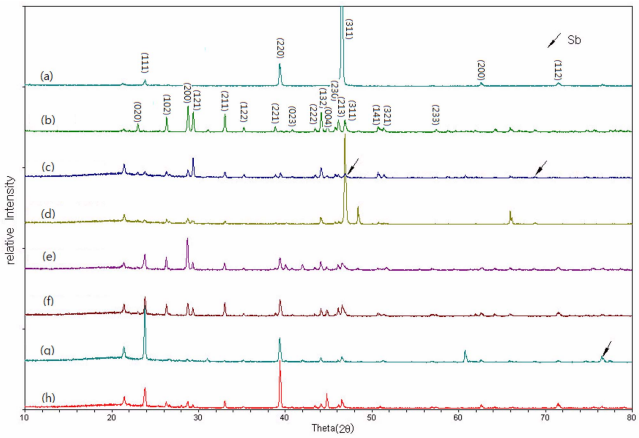

Fig. 3. X-ray diffraction patterns of the ZnSb-InSb systems ; (a) InSb, (b) ZnSb, (c) 2 mol. % InSb, (d) 10 mol. % InSb, (e) 20 mol. % InSb, (f) 30 mol. % InSb, (g) 40 mol. % InSb, (h) 50 mol. % InSb.

from the remaining melt. In the ZnSb-CdSb systems, the annealing of the sample causes the decomposition of the eutectic system and the formation of a three-phase ZnSb+ CdSb+$(ZnSb)_x(CdSb)_y$ system.[14] It is believed that melts of the ZnSb-InSb system may solidify in a similar manner.

3.2. Thermoelectric properties

Figure 6 shows the temperature dependence of the thermoelectric properties and dimensionless figure of merit (ZT) of ZnSb-GaSb systems containing 0 mol. % to 50 mol. % GaSb between 323 K and 623 K. The Seebeck coefficient of the ZnSb-GaSb systems (Fig. 6(a)) tends to increase monotonously with temperature. The Seebeck coefficient of ZnSb increased from 114 μVK^{-1} at 323 K to 226 μVK^{-1} at 623 K but decreased as the GaSb mole percentage increased to 50 mol. % GaSb, with the exception of ZnSb-20 mol. %GaSb. More detailed study is needed to understand why the See-

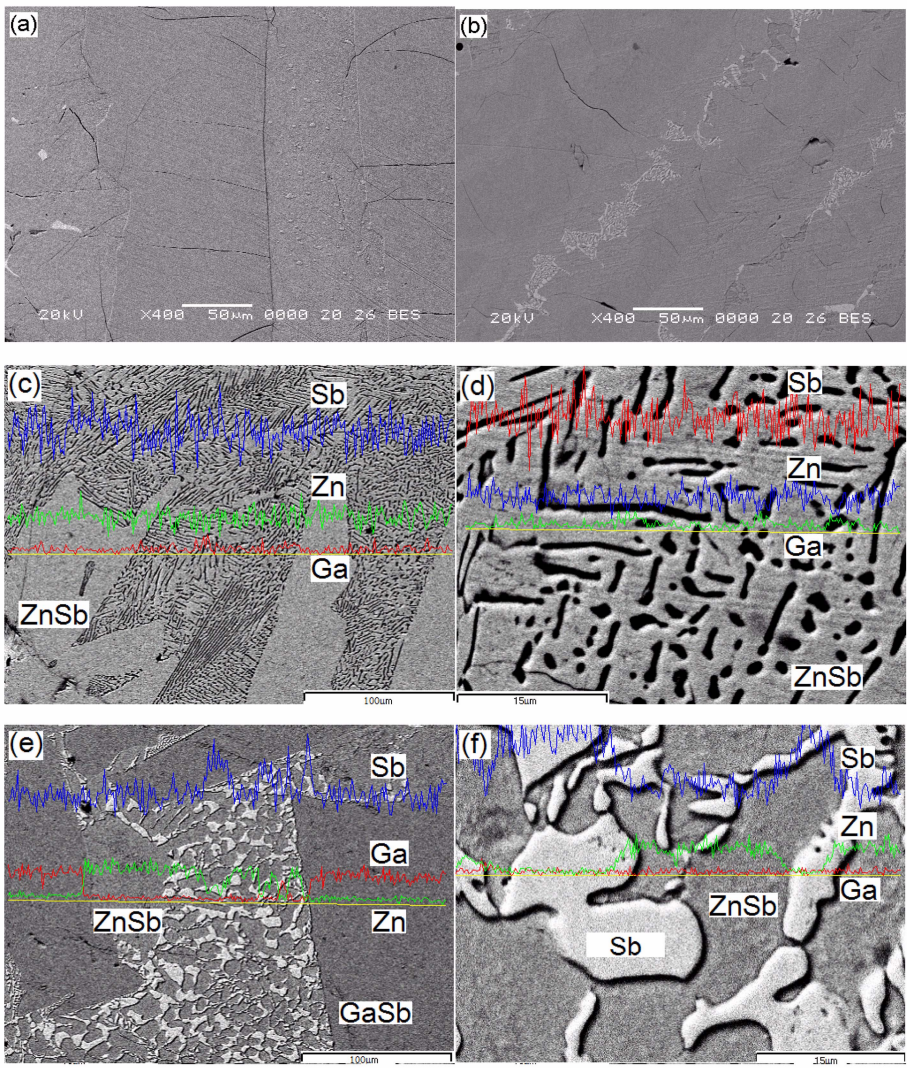

Fig. 4. Microstructures and EDS analysis results of the ZnSb-GaSb systems; (a) 1 mol. % of GaSb, (b) 3 mol. % GaSb, (c) and (d) 5 mol. % GaSb, and (e) and (f) 40 mol. % of GaSb.

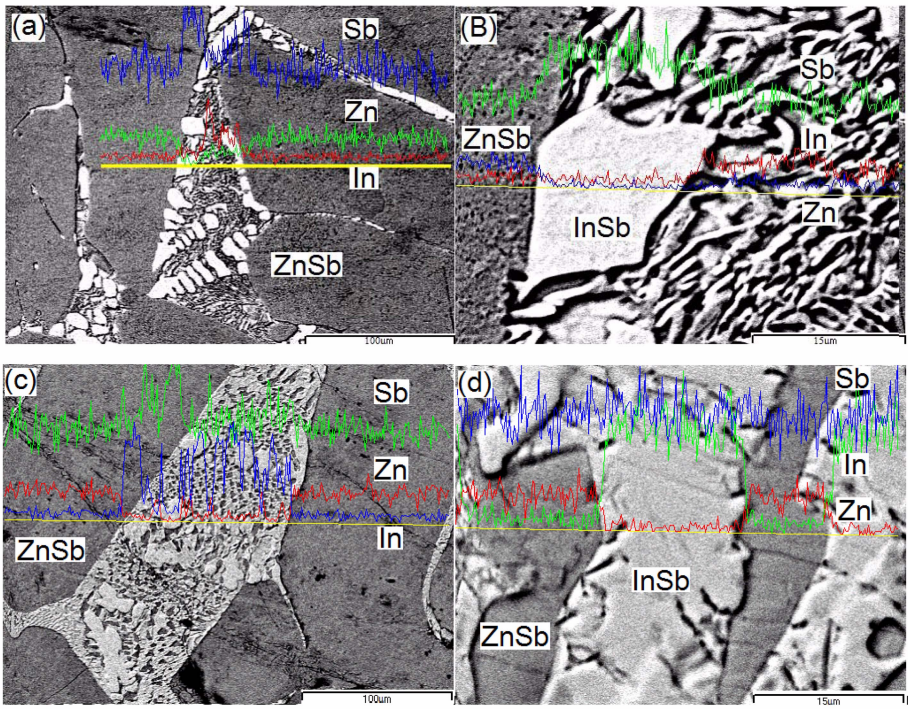

Fig. 5. Microstructures and EDS analysis results of the ZnSb-InSb systems; (a) and (b) 2 mol. % of InSb, and (c) and (d) 10 mol. % of InSb.

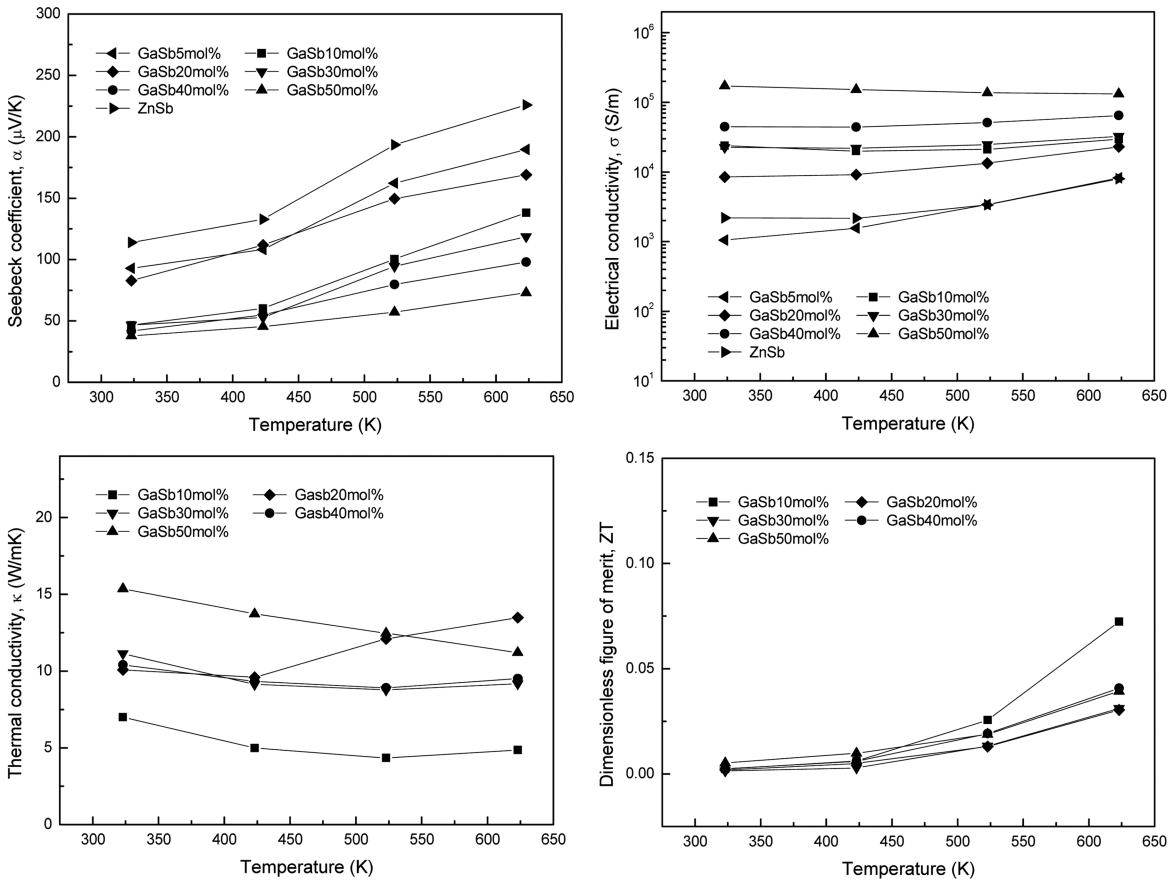

Fig. 6. Temperature dependence of the thermoelectric properties of the ZnSb-GaSb systems.

beck coefficient of ZnSb-20 mol. %GaSb is higher than that of ZnSb-10 mol. %GaSb. The electrical conductivity of ZnSb-GaSb systems other than ZnSb-50 mol. %GaSb (Fig. 6(b)) has typical semiconducting characteristics: it increases linearly as the temperature increases from 323 K to 623 K. With a low acceptor concentration, the transition to the region of intrinsic conductivity in pure ZnSb occurs at 300 K.[15] The metallic conduction behavior of ZnSb-50 mol. %GaSb suggests that a metallic Sb phase, which can be confirmed by XRD (Fig. 2) and EDS (Fig. 4), affects the electrical conductivity. In contrast to the Seebeck coefficient, the electrical conductivity increases as the GaSb mole percentage increases. The Seebeck coefficient and electrical conductivity appear to show this tendency because of complex effects, such as the volume fraction increase in the GaSb phase, the existence of a metallic Sb phase, and the doping effect from the dissolution of Ga atoms in the ZnSb phase or Zn atoms in the GaSb phase. As shown in Fig. 7, the carrier concentration of ZnSb is 3.29×10^{18} cm^{-3}. The carrier concentration increases as the GaSb mole percentage increases and becomes 4.96×10^{20} cm^{-3} in ZnSb-50 mol. %GaSb. However, the carrier mobility decreases, possibly because GaSb causes an increase in electron scattering. The thermal conductivity of the ZnSb-GaSb system (Fig. 6(c)) tends to decrease linearly as the temperature increases from 323 K to 623 K (with the exception of ZnSb-20 mol. %GaSb, which increases). Although the electrical conductivity increases with temperature, the thermal conductivity decreases. This outcome means that the lattice thermal conductivity decreases significantly. At the interface of a two-phase mixture, phonon scattering is stronger than electron scattering. As the GaSb concentration in ZnSb increases, the thermal conductivity of ZnSb-GaSb systems at 623 K increases from 4.9 $Wm^{-1}K^{-1}$ in 10 mol. % GaSb to 11.2 $Wm^{-1}K^{-1}$ in 50 mol. % GaSb. The lattice thermal conductivity of intrinsic GaSb is approximately 33 $Wm^{-1}K^{-1}$ to 38 $Wm^{-1}K^{-1}$.[16] Therefore, the increase in thermal conductivity is due to an increase in the volume fraction of GaSb because, as shown in Fig. 4, the microstructure of the ZnSb-GaSb system with more than 3 mol. % GaSb consists of a mixture of each phase. Figure 6(d) shows the GaSb addition affects the ZT value of ZnSb-GaSb systems. The ZT value reached a maximum of 0.03 in ZnSb-10 mol. %GaSb at 623 K due to the lowest thermal conductivity between the systems.

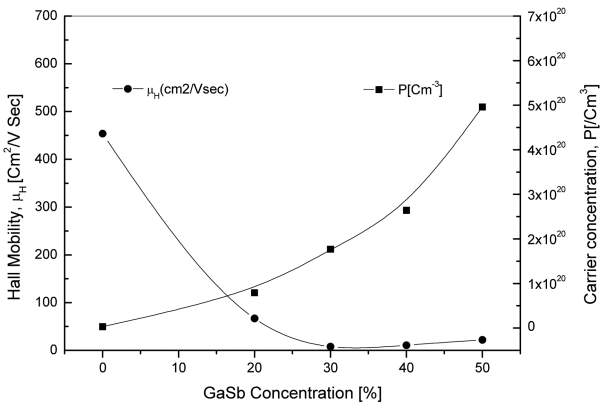

Fig. 7. Hall Mobility and carrier concentration of the ZnSb-GaSb systems.

Figures 8(a) to (c) show the temperature dependence of the thermoelectric properties of ZnSb-InSb systems, and Fig. 8(d) presents the thermal conductivity and ZT value of ZnSb-2 mol. %InSb. The Seebeck coefficient (Fig. 8(a)) of ZnSb-InSb systems, (other than ZnSb with 40 mol. % InSb), tends to increase as the temperature increases and reaches a maximum of 194 μVK^{-1} in ZnSb-2 mol. % InSb at 623 K. However, in the case of ZnSb-40 mol. %InSb, there is little temperature dependence above 423 K. The change in the Seebeck coefficient is not consistent with the addition of InSb; it decreases to a minimum of 40 μVK^{-1} to 73 μVK^{-1} at ZnSb-10 mol. %InSb when the InSb concentration is increased to 10 mol. %. The Seebeck coefficient increases when the InSb concentration is increased to 30 mol. % but then decreases at higher concentrations. The way the electrical conductivity (Fig. 8(b)) changes in relation to mole percentage of InSb contrasts with the way the Seebeck coefficient changes. As shown in Fig. 5, this behavior is attributed to an increase in the volume fraction of the InSb phase until InSb reaches 10 mol. %. The electrical conductivity of intrinsic InSb is reportedly 22,000 Sm^{-1} at 300 K and 220,000 Sm^{-1} at 773 K.[17] These values are one to two orders of magnitude higher than the electrical conductivity (2,200 Sm^{-1} to 8,000 Sm^{-1}) of the ZnSb found in this study. As shown in Fig. 8(c), the thermoelectric power factor of the ZnSb-InSb systems reaches a maximum of 0.7 $mWm^{-1}K^{-2}$ at 623 K in ZnSb-10 mol. %InSb. On the other hand, ZnSb-20 mol. %InSb reaches a slightly higher value until 523 K. For ZnSb-2 mol. %InSb, as shown in Fig. 8(d), when the temperature increases, the thermal conductivity decreases and the dimensionless figure of merit (ZT) increases.

4. SUMMARY

This study examines the possibility of a solid solution formation in GaSb-ZnSb and ZnSb-InSb binary systems; it also examines how the alloying of GaSb and InSb up to 50 mol. % affects the thermoelectric properties of ZnSb. In the ZnSb-GaSb systems, diffraction peaks for GaSb occur with GaSb concentrations greater than 3 mol. % but not with GaSb concentrations of less than 1 mol. %. The Seebeck coefficient of ZnSb-GaSb systems tends to increase monotonously as the temperature increases and to decrease as GaSb mole percentages increases, (except in the case of ZnSb-20 mol. % GaSb). The electrical conductivity of ZnSb-GaSb systems other than ZnSb-50 mol. %GaSb has typical semi-

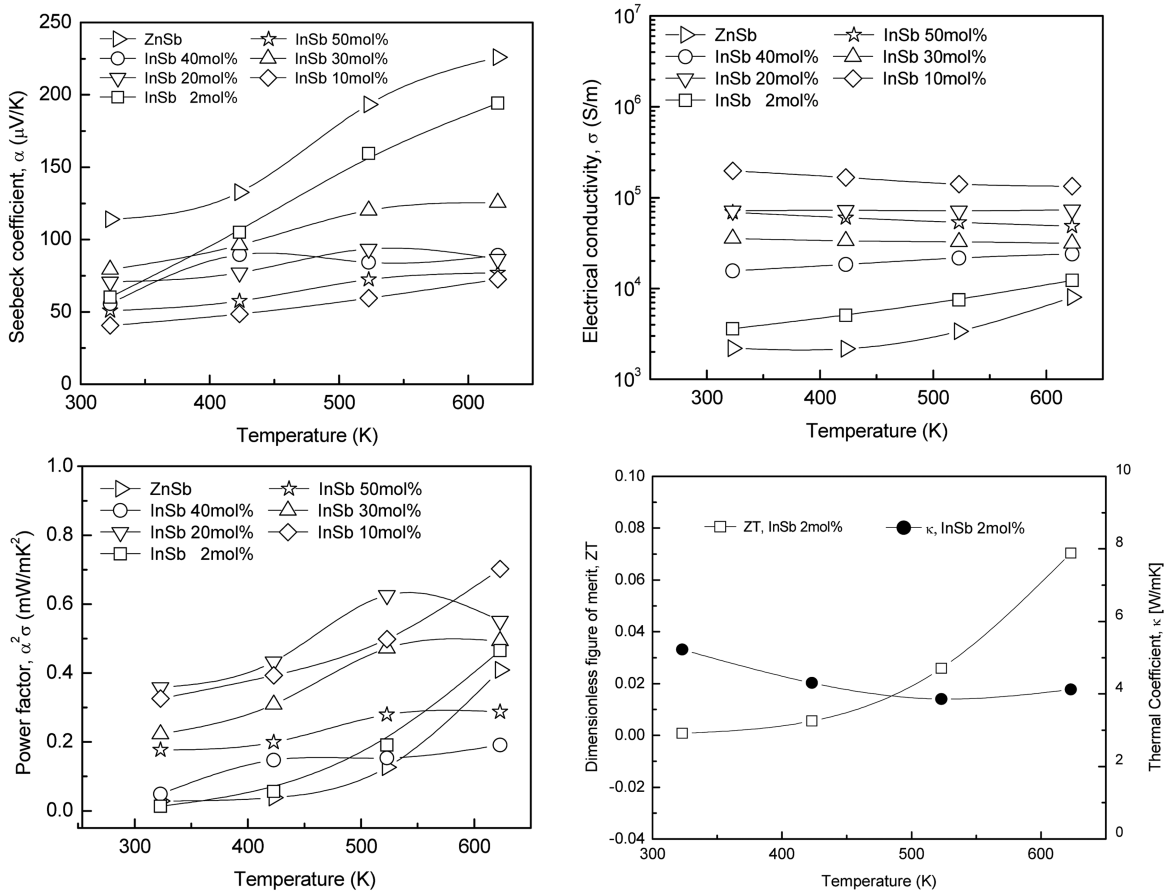

Fig. 8. Temperature dependence of the thermoelectric properties of the ZnSb-InSb systems.

conducting characteristics and increases as the GaSb mole percentage increases. The ZT value reached a maximum of 0.03 in ZnSb-10 mol. % GaSb at 623 K due to the lowest thermal conductivity (4.9 $Wm^{-1}K^{-1}$) between the systems. The Seebeck coefficient of the ZnSb-InSb system (other than ZnSb with 40 mol. % InSb) tends to increase as the temperature rises to a maximum of 194 μVK^{-1} at 623 K in ZnSb-2 mol. % InSb. The Seebeck coefficient increases until 30 mol. % InSb and decreases at higher concentrations. The change in electrical conductivity with InSb mole percentage contrasts with that observed with the Seebeck coefficient. The thermoelectric power factor of the ZnSb-InSb systems reached a maximum of 0.7 $mWm^{-1}K^{-2}$ at 623 K in ZnSb-10 mol. % InSb.

REFERENCES

1. V. I. Psarev, I. V. Psareva, and V. G. Kirii, *J. Russ. Phys.* **27**, 753 (1984).
2. R. L. Eisner, R. Mazeisky, and W. A. Tiller, *J. Appl. Phys.* **32**, 1833 (1961).
3. P. J. Shaver and J. Blair, *Phys. Rev.* **141**, 649 (1966).
4. K. W. Jang, I. H. Kim, J. I. Lee, and G. S. Choi, *Proc. Intl. Symp. Adv. Cer. Technol. Sustainable Energy App*., (ed., J. L Huang), p. 119, CSMS, Kenting. Taiwan (2007).
5. K. Tolman, *J. Chem. Sol.* **11**, 342 (1959).
6. S. Schlecht, C. Erk, and M. Yosef, *Inorg. Chem.* **45**, 1693 (2006).
7. M. Olivier and F. Werner, *J. Electrochim. Acta* **53**, 518 (2007).
8. R. Venkatasubramanian, (A.C. Pezzi) KAPL-P-000153 (1977).
9. L. S. Palatnik, G. V. Fedorov, L. A. Kornienko, A. F. Bogdanova, and A. L. Toptygin, *J. Russ. Phys.* **11**, 37 (1968).
10. K. Akai, H. Kurisu, T. Shimura, and M. Matsuura, *Proc. 23th Intl. Conf. Thermoelectrics*, (ed., J. Rüttgers), p. 334, IEEE, Dresden, Germany (1997).
11. A. S. Mikhaylushkin, J. Nylén, and U. Häussermann, *Chem. Europ. J.* **11**, 4912 (2005).
12. V. Izard, M. C. Record, and J. C. Tedenac, *J. Alloys Compd.* **345**, 257 (2002).
13. T. A. Kostur and V. I. Psarev, *Izvestiya VUZ Fizika* **12**, 118 (1969).

14. Yu. P. Keloglu and A. S. Fedorko, *J. Sov. Phys.* **13**, 977 (1970).
15. L. Mlnaříková, A. Tříska, and L. Štourač, Czechoslovak, *J. Phys.* **20**, 63 (1970).
16. D. P. Spitzer, *J. Phys. Chem. Sol.* **31**, 19 (1970).
17. J. H. Westbrook, *Intermetallic Compounds* (ed., R. E. Krieger), p. 525, Publishing Company Huntington, New York (1977).